ELSEVIER

Comput. Methods Appl. Mech. Engrg. 164 (1998) 207–221

Computer methods in applied mechanics and engineering

Some efficient boundary integral strategies for time-harmonic wave problems in an elastic halfspace

Lingyun Pan[a,*], Frank Rizzo[a], P.A. Martin[b]

[a]*Department of Aerospace Engineering and Engineering Mechanics, Iowa State University, Ames IA 50011, USA*

[b]*Department of Mathematics, University of Manchester, Manchester M13 9PL, UK*

Abstract

When Boundary Integral Equation/ Boundary Element Methods (BIE/BEMs) are used for halfspace problems, such as occur frequently in elastodynamics, the fullspace (Stokes) fundamental solution or halfspace (Lamb) fundamental solution can be used to formulate the BIE. Both Stokes and Lamb approaches have advantages and disadvantages. This paper presents systematic strategies, based on the BEM for 3D halfspace elastodynamic problems, wherein the best features of formulations based on the Stokes and the Lamb solutions are exploited. Strategies are illustrated and numerical results are given for point sources and radiation from a spherical void in a halfspace.

1. Introduction

Boundary Integral Equation/Boundary Element Methods (BIE/BEMs) have proven to be powerful tools for formulating and numerically attacking exterior boundary value problems. In this paper the BIE method refers to the formulation of a problem in terms of integral equations defined on the boundaries of a domain. The BEM refers to the procedure used to discretize the integral equations, using boundary elements, and the procedure used to solve the integral equations numerically. These tools have certain advantages over domain-based numerical methods for such problems. With the (radiation) conditions on the surface at infinity incorporated analytically, only finite surface(s) need to be discretized when the only other surface(s) in the problem are finite in extent. With domain-based numerical methods, such as the finite element method, element-modeling of an entire infinite domain is, of course, impossible. Simply truncating the finite-element model of the infinite domain is usually inadequate. Thus, special features are introduced into these methods to model such a domain and to satisfy the radiation condition [1].

However, when a BEM is used for halfspace problems, such as occur frequently in elastodynamics, and the fullspace (Stokes) fundamental solution is used to formulate the BIE, a truncated discretized model of the halfspace *surface* is required. (Usually, a discretized model of a finite surface, such as a buried finite obstacle, is needed as well.) Therefore, a truncation problem can exist in modeling a halfspace problem, even with boundary methods. However, with Stokes and the BEM, the truncation issue is different than with, say, finite elements. With finite elements the domain itself and not just a bounding surface must be truncated; thus the nature of each kind of truncation is different in a very basic way. Indeed, a good boundary solution can usually be obtained with the BEM even with severe truncation of the halfspace surface. This truncation may be simple, i.e. no special layer of 'infinite' elements to simulate the 'rest of the halfspace surface' need be used.

Alternatively, if the BEM procedure uses the Lamb fundamental solution, which models the complete halfspace surface analytically, no truncation issues even arise. But, since Lamb's solution is available in an

* Corresponding author. Currently work for Automated Corporation, 423 S.W. Washington, Peoria, IL 61602, USA.

0045-7825/98/$19.00
PII: S0045-7825(98)00055-3

analytical form which requires (numerical) evaluation of infinite integrals with respect to frequency, the CPU time spent on just forming a boundary integral equation is increased significantly and often prohibitively. Further, for some combination of locations of source point and field point, it is especially difficult or, with certain algorithms, impossible to evaluate the Lamb solution.

Problems of radiation and scattering in a halfspace have been under investigation via BIE/BEM for some time. In the time domain, the BIE has been used for halfspace dynamics problems [2,3] for linear and nonlinear problems. In both studies, the Stokes solution was employed, and discretization over the halfspace surface was required. In the frequency domain, the BIE was used for the foundation problems in a halfspace [4] for studying the dynamic response of rectangular foundations. Again, the Stokes solution was used, and a truncation on the halfspace surface was needed. However, in [5] and [6] the Lamb solution was used to formulate the axisymmetric BIE for a layered viscoelastic halfspace to avoid discretization of the halfspace surface. A BIE formulation using Lamb's solution for elastic halfspace problems, free from principal-value integrals, was proposed in [7]. In a follow-up study [8], halfspace problems were considered by BIE formulations using both Stokes' and Lamb's tensors. Comparisons were done by checking boundary solutions obtained with both kernels. However, truncation effects on the boundary solution, as well as on the solution for interior points were not addressed.

In summary, all of the researchers cited above attacked the halfspace problem by the BIE either by using the Stokes solution, making a truncated discretization on the halfspace surface, getting a fairly good solution on the boundary, or by using the Lamb solution without concern for computational efficiency. Several questions arise then regarding the BEM for halfspace problems; such as, can good results be obtained everywhere by using the Stokes solution alone? Is it always better to just use the BIE formulation using the Lamb solution? Is there a way to take advantage of both formulations to attack halfspace problems if questions of practicality and efficiency must govern? An attempt is made to answer these questions in this paper.

Specifically, we present systematic strategies, based on the BEM for halfspace elastodynamic problems, wherein the best features of the Stokes solution and the Lamb's solution are exploited. This research is motivated by a general class of problems related to responses due to explosions or other disturbances inside an underground structure. Here, we restrict ourselves to time-harmonic radiation problems, even though we can study scattering problems in a similar manner and can deal with transient problems through the Fourier transform and the Laplace transform [9].

Most of our strategies are illustrated and numerical results are presented for point sources in a halfspace and radiation from a spherical void in a halfspace.

2. BIE formulations

Consider a homogeneous, isotropic, elastic halfspace bounded by a flat halfspace surface at $z = 0$, which is traction free, as shown in Fig. 1. The elastic material fills the halfspace $z \geqslant 0$. There is a finite obstacle B inside

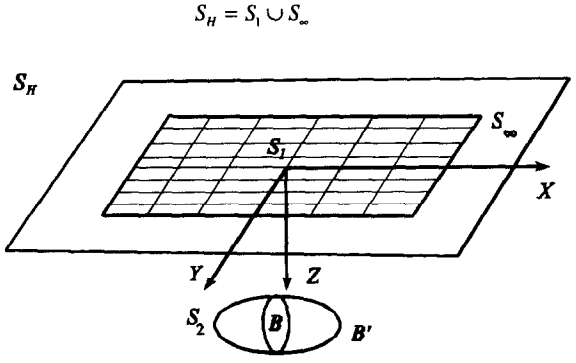

Fig. 1. The halfspace problem.

the halfspace with a surface S_2. In the region B', exterior to B but within the halfspace, we assume that an elastic field exists in the form of a time harmonic displacement vector $u_i(p,\omega)$, which must satisfy the familiar Navier equation,

$$(c_1^2 - c_2^2)u_{j,ji} + c_2^2 u_{i,jj} + \omega^2 u_i = 0 \tag{1}$$

where c_1 and c_2 are dilatational- and shear-wave speeds, respectively, ω is the circular frequency, and body forces are assumed to be zero. This field is assumed to arise from a prescription of boundary data on S_2.

Next, a Somigliana integral formula based on the Stokes point force solution may be derived (see [7]), and written as

$$C_{ij}(p)u_j(p) = \int_{S_H + S_2} [T_{ij}(p, q)u_j(q) - U_{ij}(p, q)t_j(q)]\, ds(q) \tag{2}$$

in which U_{ij} and T_{ij} are Stokes' displacement and traction tensors, respectively, which describe the fields at a point q due to a time harmonic point force of frequency ω at a point p in a fullspace [7]. Here, we assume no incident wave in B' and $C_{ij}(p)$ is the coefficient tensor of the free term (again see [7]) and is a function of the location of p. When p is inside B', Eq. (2) is a representation integral which gives the solution at p in terms of boundary values of $u_j(q)$, $t_j(q)$ on both S_H and S_2, and $C_{ij}(p) = \delta_{ij}$. When p is on the boundary, either S_H or S_2, Eqn. (2) is a BIE in which half of the pair of variables $u_j(q)$, $t_j(q)$ are prescribed for a well-posed problem. The BIE (2) can be solved for the other half of the boundary data.

Indeed, in the BIE process, the first step is to put p on the boundary; the BIE is then solved for the unknown boundary data. In the second step, the solution at any point inside the domain B' can be obtained from the representation integral. In both steps, all of the integrals are evaluated numerically, so a discretization is needed on both the halfspace surface and the finite surface. Since S_H is infinite, only a truncated finite area S_1 would be discretized. Thus truncation arises when solving the BIE as well as when obtaining the solution at a field point.

Denote the neglected area on the halfspace surface as S_∞ (see, Fig. 1), i.e. $S_H = S_1 \cup S_\infty$, and for all problems of interest in this paper, $t_j(q) \equiv 0$ on S_H. Thus, the BIE equation (2) can be expanded as

$$C_{ij}(p)u_j(p) = \int_{S_2} [T_{ij}(p, q)u_j(q) - U_{ij}(p, q)t_j(q)]\, ds(q) + \int_{S_1} T_{ij}(p, q)u_j(q)\, ds(q) + \int_{S_\infty} T_{ij}(p, q)u_j(q)\, ds(q)\,. \tag{3}$$

The last term is associated with the neglected area S_∞. For p located on S_2 or S_1, and q on S_∞, we find that the contribution of this last term may be neglected without detriment to the accuracy of the boundary solution, provided S_1 has at least a minimum size. This matter is discussed in some detail in the next section.

Now if instead of the Stokes tensor U_{ij} and T_{ij}, Lamb's tensors U_{ij}^H and T_{ij}^H are used, the Somigliana integral need only be taken over S_2 because the presence of the traction-free halfspace surface is accounted for in Lamb's tensors. That is, $T_{ij}^H(p, q) = 0$, whenever q is on S_H (see [14]). Thus, the Somigliana integral formula has the simple form:

$$C_{ij}(p)u_j(p) = \int_{S_2} [T_{ij}^H(p, q)u_j(q) - U_{ij}^H(p, q)t_j(q)]\, ds(q)\,. \tag{4}$$

There is no truncation issue because the integral is taken only over the finite surface S_2. However, the computation of Lamb's halfspace Green's function for (4) as a BIE is very time consuming. To give an idea of the CPU time difference between formulating and solving the BIE using the Stokes solution, and formulating and solving the BIE again using the Lamb solution, an experiment was performed for a sphere, in a fullspace, with an 8 element discretization. It took 2.8 seconds to solve the BIE using the Stokes solution. When the Lamb solution was used, the CPU time was 820 seconds. Thus we were motivated to look carefully at the Stokes formulation despite the shortcomings, conceptually at least, of truncation.

3. Truncation study for the BIE using the stokes solution

To investigate truncation effects on boundary solutions and results at field points via Stokes, the problem of a point load in a halfspace was considered first. Displacements on the halfspace surface obtained as the boundary solution in the Stokes BIE should then be identical to the corresponding displacements given by the halfspace Green's function U_{ij}^H. Because of the absence of S_2 and the existence of the point source, the Stokes BIE (3) reduces to

$$C_{ij}(p)u_j(p) = \int_{S_1} [T_{ij}(p, q)u_j(q) - U_{ij}(p, q)t_j(q)]\, ds(q) + U_{ij}(p, p_0)F_j(p_0) \tag{5}$$

in which p_0 is the location of the point source; F_j is the magnitude or strength vector of the point source.

The point source is located at (0, 0, 1) which is one meter below the halfspace surface, and is in the z direction for all the results presented here. This makes $F_1 = F_2 = 0$, $F_3 = 1$ in Eqn. (5). In Fig. 2, we show the comparison between our boundary solutions and exact point force solutions for the magnitude and phase angle of u_1 and u_3 components along x direction on the halfspace surface. The results presented there are for a point source in titanium alloy ($c_1 = 6340$ m/s, $c_2 = 3030$ m/s, Poisson's ratio $\nu = 0.352$) when the discretized area S_1 is chosen as a 24×24 square area. (Later, we will show that a much smaller discretized area S_1 can be used to obtain a good solution.) The shear wave number is $k_t = 0.449$ (which corresponds to frequency $\omega = 1360$ Hz), The discontinuity in the phase-angle plot is caused by the jump in $+180°/-180°$. Note that the validity of our BEM analysis is confirmed by the good agreement between our computed results and that given by the analytical solution U_{ij}^H.

For the same point force, in the same material at the same frequency, we show, in Fig. 3, the variation of the magnitude of field u_3 along the x direction for four different sizes of the discretized area $2L \times 2L$ of $L = 3, 4, 6, 12$, respectively, over the halfspace surface. Again, analytical data obtained from U_{ij}^H are also shown in Fig. 3 as the solid line for reference. Note that data points obtained via our BEM, for four different sizes of truncation, represented as '×', '*', 'O', '+', respectively, all fall equally well on the reference curve. This is an important observation. It suggests that very good results can be obtained by using a relatively small ($L = 3$) discretized model S_1 of S_H. The main effect of a larger S_1 is to obtain additional surface data over the added-discretized portion of S_H. However, the increase in accuracy of the boundary values of u_3 over a given model of S_H, by making that model larger, seems to be negligible.

We tested these observations at several higher frequencies up to a k_t of 2.245. We found that the observations held up. There was deterioration in the data with increasing frequency as expected, but that was attributable to the fact that the boundary element size (which was held constant with changes in L and frequency) became larger than the four-elements-per-wavelength known to be needed in the frequency range being examined. The important thing is that larger L yielded data no better nor no worse than smaller L at a given frequency and element size.

On the other hand, we do know that there are different L requirements, in general, for different depths d of a disturbance. Although the magnitude of the surface disturbance decreases with increasing d, we have observed that larger L is required to accurately pick up the decreased surface disturbance on the modeled portion S_1 of S_H, as d increases. Moreover, how interior u (field data) might depend on the size of L, for any depth of disturbance, is another question. Both of these issues, i.e., the size of L needed: (i) as a function of depth of source of a disturbance, and (ii) as a function of location of the desired field, are considered further subsequently.

In general, observations made about data from point source results are very important because the radiation from any kind of a shape in the halfspace could be viewed as the radiation by a distribution of point sources. To confirm this, we studied the radiation from a spherical void which is used to simulate a spherical wave in the halfspace.

Consider a spherical cavity of radius r the center of which is buried a distance d inside a homogeneous, elastic half-space and which is radiating harmonic dilatational waves into the halfspace, such that $t_r = 1.0$, $t_\theta = t_\phi = 0.0$. Since the magnitude of spherical waves decreases with distance from the source, the reflected waves due to the presence of the halfspace surface also have a diminishing effect as they travel through the medium. Thus, it is expected as the distance d increases, the surface data on the sphere should approach the corresponding fullspace solution. This observation can be viewed as a check for the algorithm and coding (analytical comparison data are not available for this problem), and the expected behavior is apparent from Fig.

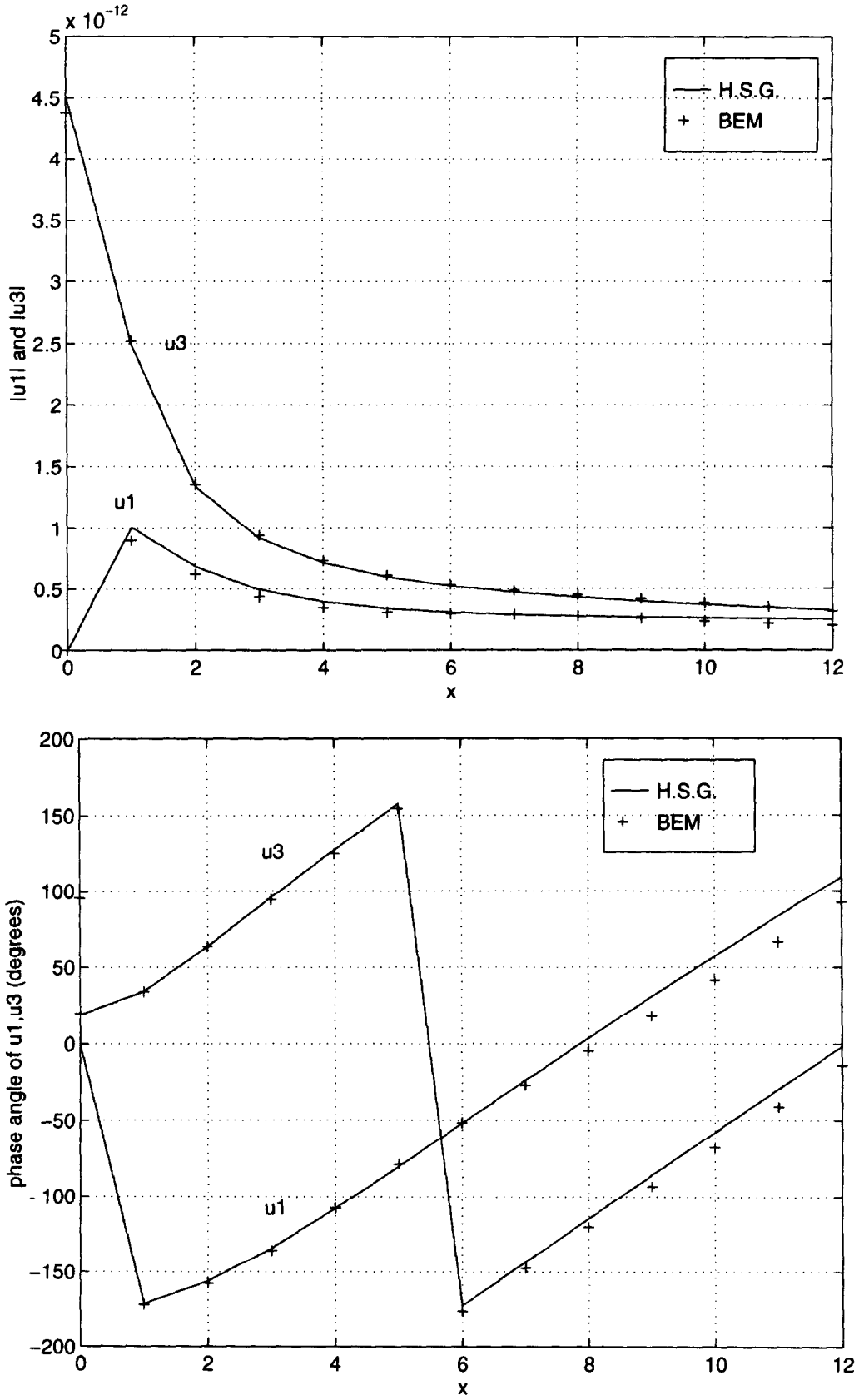

Fig. 2. Comparison of boundary solutions from $L = 12$ discretization with Lamb's solution for point loading ($d = 1$).

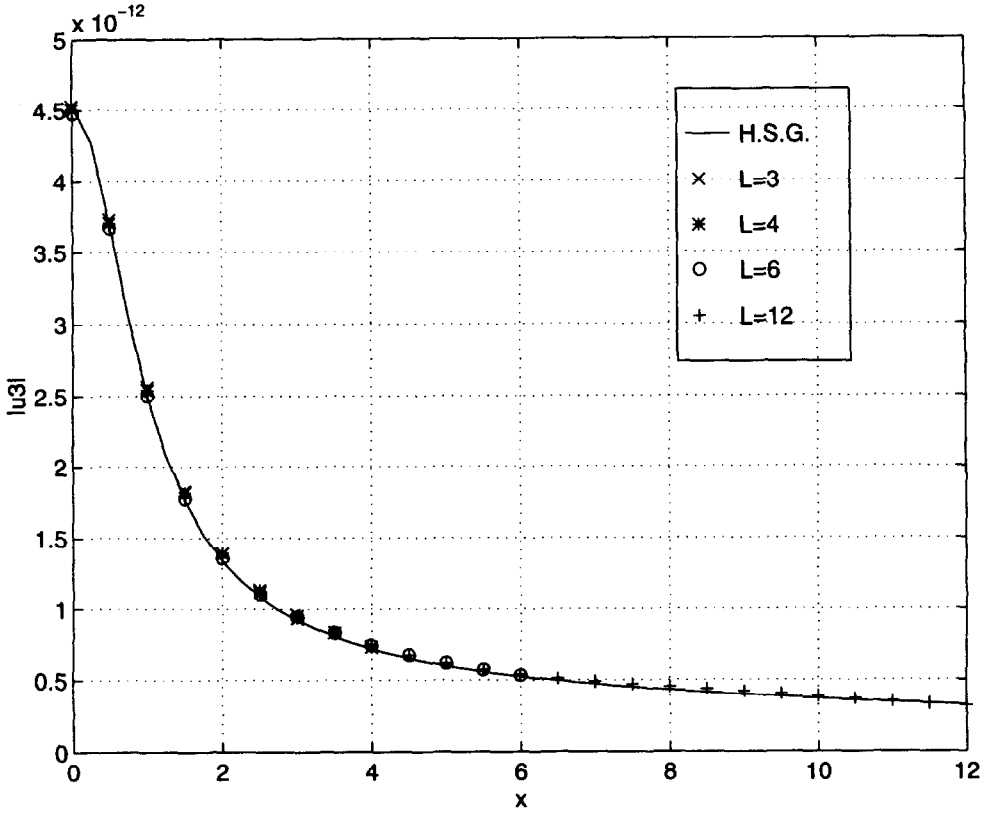

Fig. 3. Truncation effect of point source response ($d = 1$).

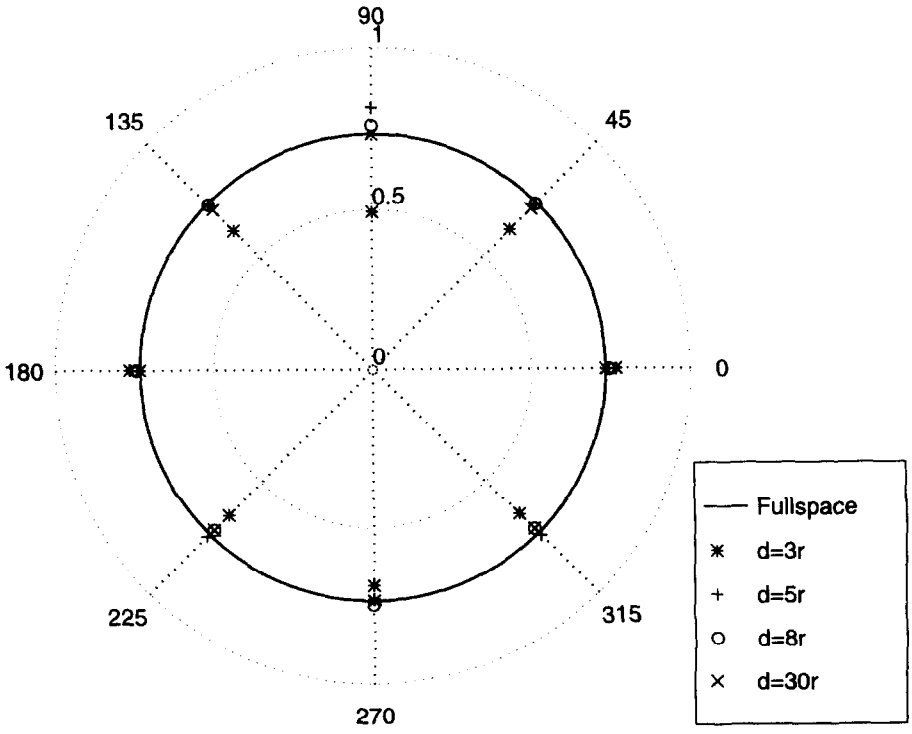

Fig. 4. Polar plot of $|u_r|$ for radiation from a spherical void.

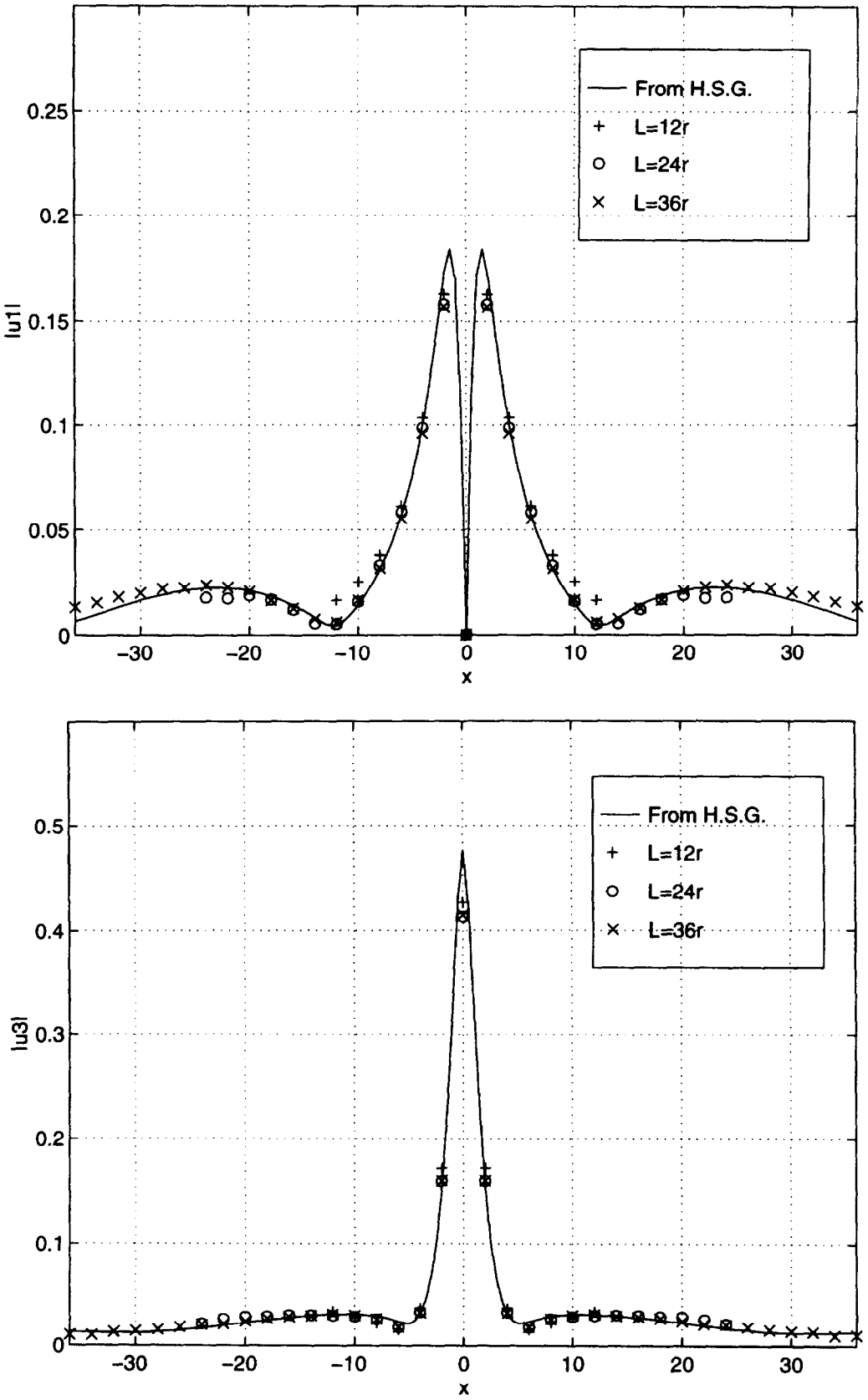

Fig. 5. Truncation effect for radiation from a spherical void ($d = 2r$).

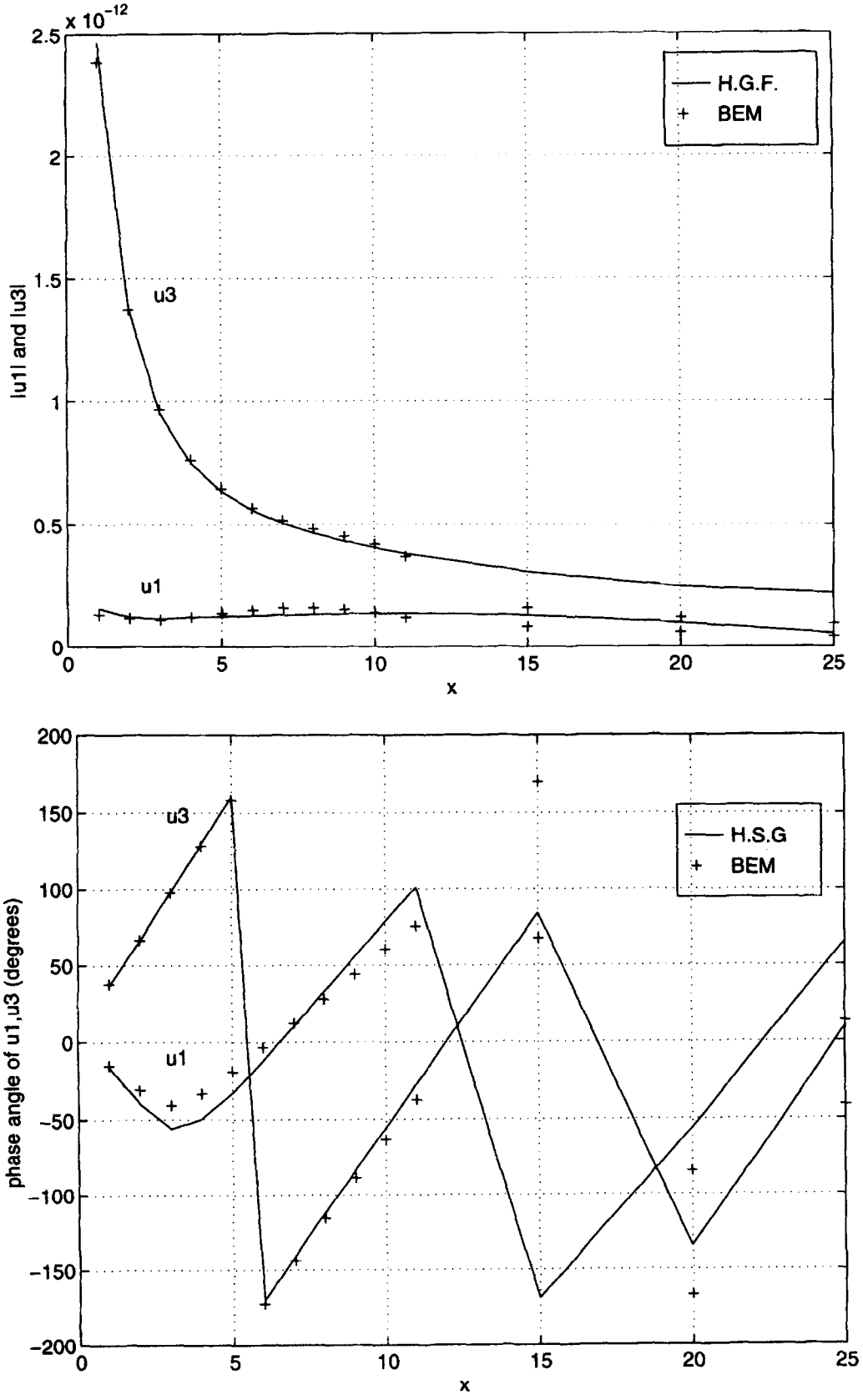

Fig. 6. Field values at interior points (point load).

4, in which there is a polar plot of the magnitude of the radial displacement component on the sphere surface and on plane $y = 0$ for several different depths of the sphere when $k_p r = 0.913$ (k_p is the dilatational wave number), and Poisson's ratio $\nu = 0.25$. The solid circle is the solution for a radiating sphere in the fullspace. Points '*', '+', 'O', '×' represent our BEM solution at eight angular positions for a radiating sphere located in a halfspace at $d = 3r$, $d = 5r$, $d = 8r$, $d = 30r$, respectively. The BEM data are obtained by solving the BIE with Lamb's solution, i.e. Eq. (4). The trend that as d increases, the solution at all eight data points along the circumferential direction all go correspondingly closer to the circle, indicates the correctness of the algorithm and coding. It can be seen when $d \geq 8r$, the surface data are quite close to the corresponding fullspace solution. Thus, for sufficiently large d, it may be possible to avoid discretization of S_H altogether (See Section 6 below, especially Fig. 8).

Returning to $d = 2r$, Fig. 5 shows the variation of u_1 and u_3 components on the halfspace surface obtained using three different sizes of discretization $2L \times 2L$ on the S_H surface for $k_t = 0.449$. The solid line is obtained by first solving for the boundary displacements on the surface of the sphere by means of Eq. (4). Then, as a second step, the boundary integral representation is used for finding the displacements on the halfspace surface. Note only the surface of the sphere needs to be modeled since Lamb's solution is used both in the BIE equation (4) and the boundary integral representation. There is no truncation issue related to the solid line in Fig. 5. Notice that, when the BIE formulation with Stokes' solution and a truncated model on the halfspace surface are used, the calculated boundary data points on the halfspace all fall on the solid line. As in Fig. 3, it is again very clear that we pick up more information as we increase the size of the discretization. However, values of new data compared with values of previously-obtained data again show little change.

The situation for interior points is, however, different. Calculation for u_1 and u_3 at various interior point locations, for the largest discretization of S_H, were performed and compared to the analytical solution for the point load case. The general conclusion, for interior points, is that we can obtain good results for points only under the 'shadow' of the halfspace discretization. Fig. 6 shows the result for interior point samples one unit below the halfspace surface from $x = 2$ to $x = 25$ due to the point load in the halfspace. It can be seen that beyond $x = 10$ the result from BEM deviates considerably from the Lamb solution. We expect results to be even worse for deeper sample points and for deeper sources of disturbance.

Therefore, while we can obtain very satisfactory boundary data over the discretized surfaces with reasonable truncation of S_H, via the Stokes BIE, we cannot obtain satisfactory field data at distances much beyond the edge of the truncated S_H. It is obviously impractical to use ever-larger models of S_H just to get desired field data at large distances from the sources of disturbance. Thus, what can be done?

4. Lamb's formulation revisited

We mentioned earlier that using the Lamb solution in forming and solving a BIE would be prohibitive for any problem requiring a substantial amount of discretization over S_2 because of the CPU time involved to get function evaluations for the many p-Gaussian quadrature point combinations involved. Note, we speak of prohibitive CPU time despite the fact that discretization of (a portion of) S_H is not even an issue with Lamb. However, suppose we get good boundary displacements over S_2 with a fairly small discretization (reasonable truncation) of S_H, as we have shown that we can do. Then, if we ask for field data, remote from S_2, via Eq. (4) used as a representation integral for comparatively *few* points p, the costs are very reasonable indeed. In fact, we may view this as an ideal compromise, the best of both worlds in a sense: specifically, use Stokes, with a reasonable truncation of S_H, to form and solve the relevant BIE; thus obtain $u_j(p)$ on S_2 accordingly, efficiently, and in reasonable time; then use Lamb in the representation integral to get the farfield data which requires boundary data over S_2 only. A similar strategy was used in [15] for scattering from a halfspace surface-breaking crack problem.

Fig. 7 shows the interior results calculated by using Stokes in the BIE and using Lamb in the representation integral (indicated by +) compared with the results from using Lamb's solution in both the BIE and the representation integral. Also in Fig. 7 is the uncorrected results if Stokes is used both in the BIE and in the representation integral. Note we used a frequency ($k_t = 1.58$) which is almost three times higher than the original one for Figs. 6, 7 and 8. The proposed Stokes-plus-Lamb strategy still works fine. It is very obvious that

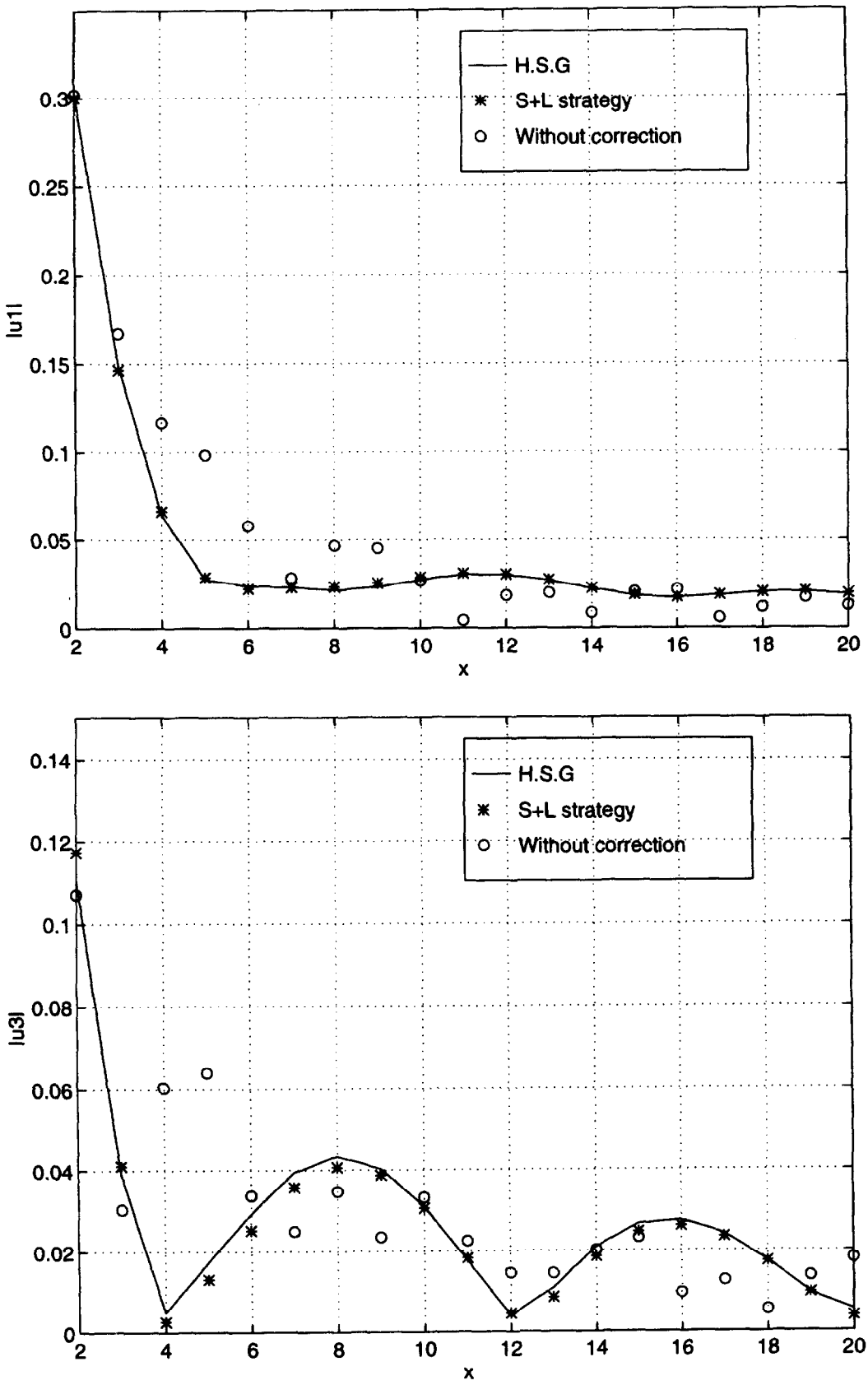

Fig. 7. Results from strategy proposed in this paper for interior points (for radiation from a spherical void).

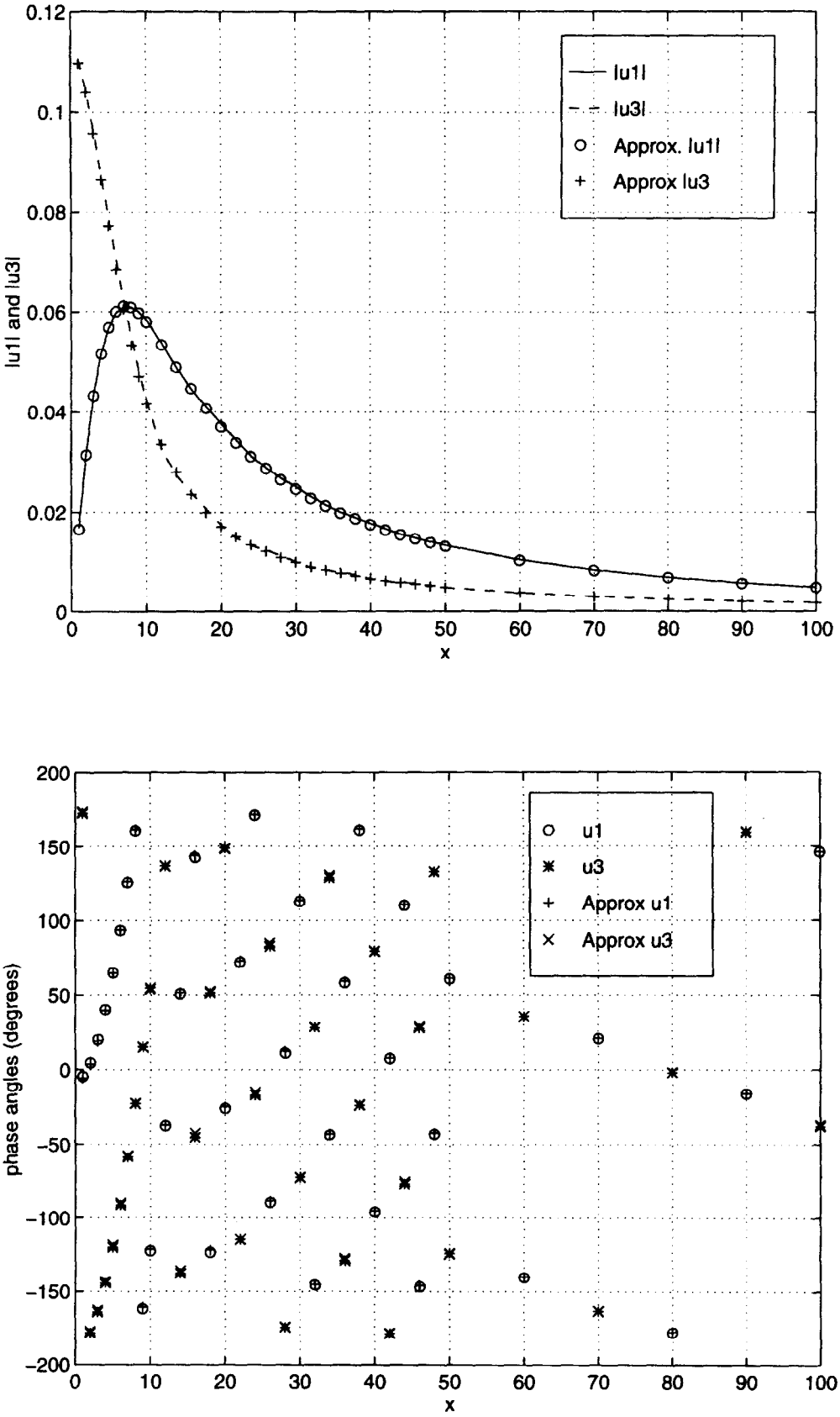

Fig. 8. Results by using large depth approximation (for radiation from a spherical void).

those uncorrected results denoted by circles deviate from the good results even for field points which are close to the origin.

5. A more efficient and faster strategy: the library

The efficiency of using the Stokes-plus-Lamb strategy described above can be improved by incorporating the idea of a 'Green's function Library' (see [11,12]). For problems with two surfaces as the boundary, such as halfspace problems (S_2 plus S_H), a sub-matrix of the coefficient matrix is the essential part of the partial Green's function for the problem. The library idea is closely related to partitioning of the system matrix.

The BIE in discretized form for the halfspace problem, using the Stokes tensors, can be written as

$$\begin{bmatrix} A_{11} & A_{12} \\ A_{21} & A_{22} \end{bmatrix} \begin{Bmatrix} u_1 \\ u_2 \end{Bmatrix} = \begin{Bmatrix} f_1 \\ f_2 \end{Bmatrix} \tag{6}$$

where A_{11} are coefficients related to collocation (source point p) on S_1, and integration (integration point q) on S_1; A_{12} are coefficients related to collocation on S_1 and integration on S_2; A_{21} are coefficients associated to collocation on S_2 and integration on S_1; A_{22} are coefficients associated to collocation on S_2 and integration on S_2; In recent papers [11,12], it has been shown that A_{11}^{-1} is in fact the essential ingredient in a 'discretized Green's function' for the halfspace problem.

Indeed, suppose we attempt to solve this system of equations via partitioning, i.e. form A_{12}, A_{21}, and A_{22} and write the following reduced system of equations:

$$(A_{22} - A_{21}A_{11}^{-1}A_{12})\{u_2\} = \{f_2 - A_{21}A_{11}^{-1}f_1\}. \tag{7}$$

Then, obtain u_1 by

$$\{u_1\} = A_{11}^{-1}\{f_1 - A_{12}u_2\}. \tag{8}$$

Further, suppose that the discretization on the halfspace surface is bigger than the discretization on the finite surface. The size of A_{11} is then much bigger than the size of A_{22}. The most computationally intensive part of the solution via Eqs. (7) and (8) then is the formation and inversion of A_{11}. This leads to the idea of making an accurate discretization of the halfspace surface, obtaining A_{11}^{-1}, and storing this large matrix so that it can be reused over and over again with different S_2. This idea is becoming attractive as storage and retrieval of mass-amounts of data become easier and cheaper. Also, only the boundary data on S_2 is of interest when using Lamb. Thus, we do not really need to go through Eq. (8) to get u_1. In actual implementation, the matrix saved is not the inverse of A_{11}, but the LU decomposition of A_{11}.

As an illustration of the benefits of this partitioning-library strategy, Table 1 shows some CPU times for a

Table 1
CPU time comparison for partitioning using Library idea

Method/Task	CPU time (s)
CPU time for solving the problem in one step	1920
144 elements on the halfspace surface, 8 elements on the sphere	
CPU time via Partitioning	
Form A_{11}	870
LU decomposition	866
Pre-effort (form A_{11} and save LU decomposition of A_{11})	1636
Form A_{22}, A_{21}, A_{12}	70
read LU decomposition of A_{11}	7.8
Calculate new coefficient matrix and right hand side	95.5
Solve the reduced equations	0.05
Total CPU time for partitioning	173

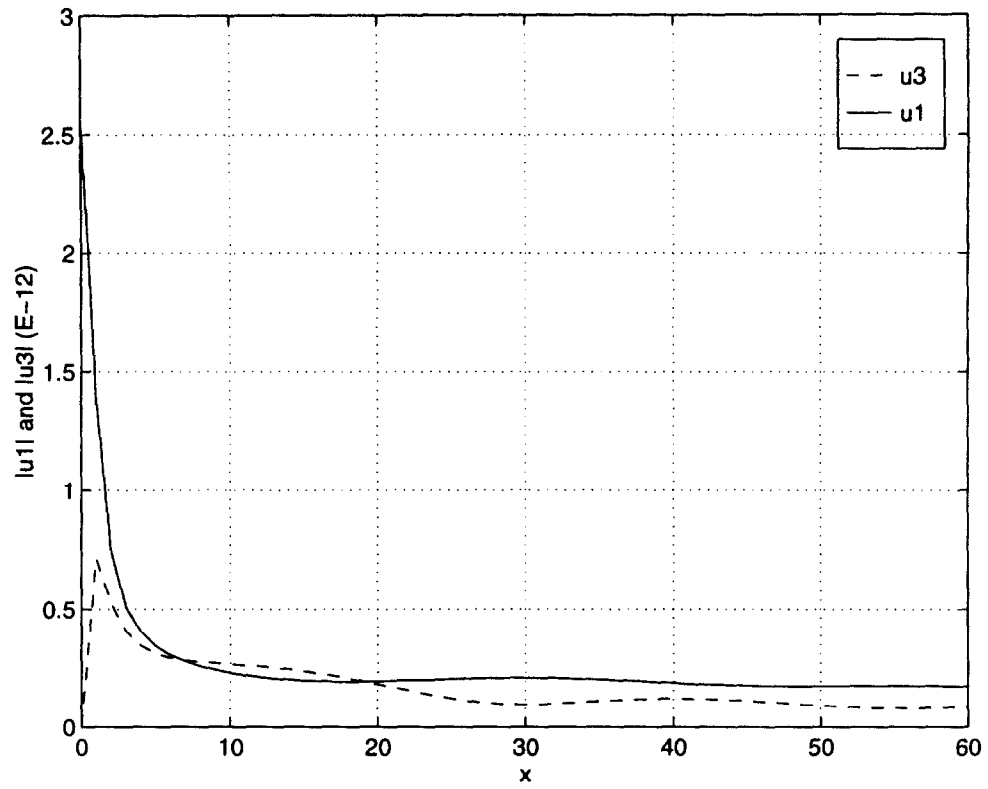

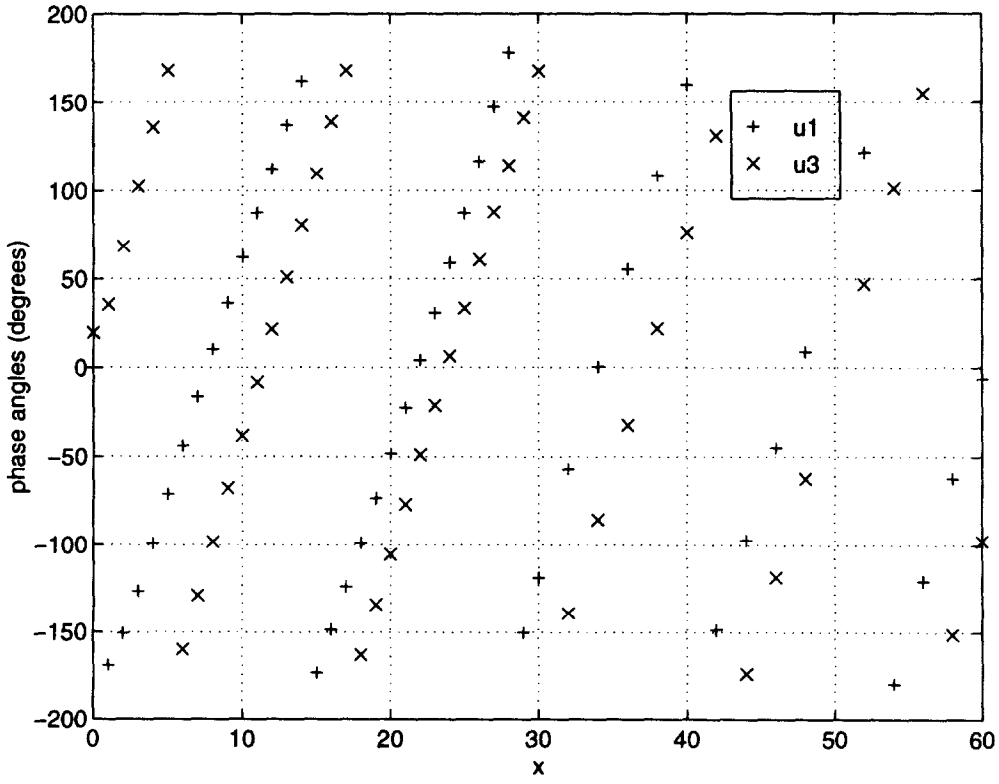

Fig. 9. Rayleigh wave features for scattered field due to point loading ($d = 1$).

typical halfspace problem solved in two ways. It can be seen that by doing partitioning, the CPU time is approximately 1/10 of the CPU time needed for solving the whole problem in one step.

6. Some useful approximations

Some useful approximations might be appropriate for the halfspace problem. First, if the finite obstacle is deep enough below the halfspace surface, we can approximate the boundary solution on the surface of the finite obstacle by solving a fullspace problem, and then this approximation gives very good results. Fig. 8 shows the interior results calculated in this way for $d = 8r$ compared with the results from using Lamb's solution. This approximation gives good results for both the magnitude and the phase angle even for farfield points. Further, we found that certain asymptotic techniques for special locations of the field points are often warranted. For example, we found that the scattered field on the halfspace surface exhibits very good Rayleigh wave features when the distance from the origin gets large. This can be seen from Fig. 9 in which the scattered field on the halfspace surface is plotted. The two main characteristics of the Rayleigh wave, i.e. the magnitude of the displacement decays very slowly and a 90° phase angle difference exists between u_1 and u_3, are very apparent. For the field caused by the radiation from a spherical void, even though the Rayleigh wave is not evident in the near field, it is found that, at certain larger distance from the origin, the scattered field also exhibits the Rayleigh wave characteristics. Thus, if the major part of the field on the halfspace surface comes from the Rayleigh wave for large distance from the origin, it is possible to use the Rayleigh wave representation and boundary solutions from the BIE to approximate the farfield on the surface. However, specific strategies for using the boundary data from BEM to construct an appropriate Rayleigh wave representation is itself an interesting topic for future research.

7. Conclusions

Both BIE formulations, i.e. via Stokes' and Lamb's solutions, are used to attack halfspace problems, and compared with each other. Each has its own advantages and disadvantages.

It is found that when Stokes is used, the halfspace-surface truncation affects both the boundary solution and the solution at field points. However, it is also found that this truncation has a small effect on the boundary values themselves, i.e. very good boundary solutions can be obtained with a small size of discretization on the halfspace surface. On the other hand, the truncation has a big effect on the results for field points, especially those field points which are out of the 'shadow' of the halfspace surface discretization. This is true even though important ingredients in the remote field point values are the truncation-insensitive boundary values. It is also found that when Lamb is used, the CPU times are usually prohibitive.

In this paper then, to counter the negative effects of truncation with Stokes and to address the excessive CPU issue with Lamb, we suggest the following: use Stokes to formulate the BIE and obtain good boundary solutions over the truncated halfspace plus a finite surface; then use Lamb's solution in the representation integral to evaluate results at field points. In this way, there are no adverse truncation effects on the results for field points, since the boundary solution on the finite surface is good, as stated, and the finite surface is the only one which must be integrated over with Lamb. For the relatively few function evaluations of Lamb's solution required in getting field point values only, CPU time is seldom a problem.

We also suggest that when using the fullspace fundamental solution in the BIE, considerable time and effort can be saved by pre-computing the coefficient matrix for the truncated halfspace surface model and storing its inverse (in reality the LU decomposition of that coefficient matrix) for repeated use. The Green's function Library idea, with the coefficient matrix for a fine discretization on the halfspace surface which is identified as the main ingredient of the partial Green's function, precomputed and stored, gives an even more efficient and faster way to attack halfspace problems.

Further, we found that certain approximations are applicable for the halfspace problem. For example, when the finite surface S_2 is deep enough below the halfspace surface, we can approximate the boundary solution on the surface of S_2 by solving a fullspace problem, and then obtaining the field in the halfspace by using Lamb's solution. Also some asymptotic techniques for special locations of the field points are often warranted. For

example, if the major part of the field on the halfspace surface comes from the Rayleigh wave, we can use the Rayleigh wave representation and boundary solutions from the BIE to approximate the farfield on the surface.

Acknowledgment

Thanks are due the Sandia National Laboratories, in Albuquerque, NM, for several communications which motivated some of this research. Many thanks are due also to Ron Roberts of the Center for Nondestructive Evaluation of Iowa State University for providing the code for calculating halfspace Green's functions and for many helpful discussions during all the phases of this project.

Finally, the authors are grateful to the Center for Computational and Theoretical Material Science of the National Institute for Standards and Technology, Gaithersburg, MD, for financial support of a portion of this research under grant No. 60NANB6D0210.

References

[1] D. Givoli, Numerical Methods for Problems in Infinite Domains (Elsevier, Amsterdam, 1992).
[2] D.L. Karabalis and D.E. Beskos, Dynamic response of 3-D embedded foundations by the boundary element method, Comput. Methods Appl. Mech. Engrg. 56 (1986) 91–120.
[3] S. Ahmad, Linear and nonlinear dynamic analysis by boundary element method, Ph.D. Dissertation, Dept. of Civil Engrg., SUNY at Buffalo, 1986.
[4] J. Dominguez, Dynamic stiffness of rectangular foundations, Research Report R78-20, Dept. of Civil Engrg., Massachusetts Institute of Technology, Cambridge, MA, 1978.
[5] R.J. Apsel and J.E. Luco, Impedance functions for foundations embedded in a layered medium: an integral equation approach, Earthquake Engrg. Struct. Dyn. 15 (1987) 213–231.
[6] F. Chapel, Boundary element method applied to linear soil structure interaction on a heterogeneous soil, Earthquake Engrg. Struct. Dyn. 15 (1987) 815–829.
[7] F.J. Rizzo, D.J. Shippy and M. Rezayat, A boundary integral equation method for time-harmonic radiation and scattering in an elastic half-space, in: T.A. Cruse, A.B. Pifko, H. Arman eds., Advanced Topics in Boundary Element Analysis, AMD-Vol. 72 (ASME, New York, NY, 1985) 83–90.
[8] I.R. Gonsalves, D.J. Shippy and F.J. Rizzo, Direct boundary integral equations for elastodynamics in 3-D half-spaces, Comput. Mech. 6 (1990) 279–292.
[9] M. Rezayat, D.J. Shippy and F.J. Rizzo, On time-harmonic elastic-wave analysis by the boundary element method for moderate to high frequencies, Comput. Methods Appl. Mech. Engrg. 55 (1986), 349–367.
[10] F.J. Rizzo, D.J. Shippy and M. Rezayat, A boundary integral equation method for time-harmonic radiation and scattering of elastic waves in three dimensions, Int. J. Numer. Methods Engrg. 21 (1985) 115–129.
[11] P.A. Martin and F.J. Rizzo, Partitioning, boundary integral equations, and exact Green's functions, Int. J. Numer. Methods Engrg. 38 (1995) 3483–3495.
[12] F.J. Rizzo, P.A. Martin, L. Pan and D. Zhang, Exact Green's functions and the boundary element method, BEM 17, 17–19 July (1995).
[13] R.A. Roberts, Elastodynamic response of contacting fluid and solid half-spaces to a three-dimensional point load, Wave Motion 12 (1990) 583–593.
[14] K. Aki and P.G. Richards, Quantitative Seismology, Vols. 1,2 (W.H. Freeman, San Francisco, 1980).
[15] D.E. Budreck and J.D. Achenbach, Three-dimensional elastic wave scattering by surface-breaking cracks, J. Acoust. Soc. Am. 86(1) (1989) 395–406.